

# ChARM: NextG Spectrum Sharing Through Data-Driven Real-Time O-RAN Dynamic Control

Luca Baldesi, Francesco Restuccia, and Tommaso Melodia  
Institute for the Wireless Internet of Things, Northeastern University, United States  
Email: {l.baldesi, frestuc, melodia}@northeastern.edu

*Abstract*—Today’s radio access networks (RANs) are monolithic entities which often operate statically on a given set of parameters for the entirety of their operations. To implement realistic and effective spectrum sharing policies, RANs will need to seamlessly and intelligently change their operational parameters. In stark contrast with existing paradigms, the new O-RAN architectures for 5G-and-beyond networks (NextG) separate the logic that controls the RAN from its hardware substrate, allowing unprecedented real-time fine-grained control of RAN components. In this context, we propose the Channel-Aware Reactive Mechanism (ChARM), a data-driven O-RAN-compliant framework that allows (i) sensing the spectrum to infer the presence of interference and (ii) reacting in real time by switching the distributed unit (DU) and radio unit (RU) operational parameters according to a specified spectrum access policy. ChARM is based on neural networks operating directly on unprocessed I/Q waveforms to determine the current spectrum context. ChARM does not require any modification to the existing 3GPP standards. It is designed to operate within the O-RAN specifications, and can be used in conjunction with other spectrum sharing mechanisms (e.g., LTE-U, LTE-LAA or MulteFire). We demonstrate the performance of ChARM in the context of spectrum sharing among LTE and Wi-Fi in unlicensed bands, where a controller operating over a RAN Intelligent Controller (RIC) senses the spectrum and switches cell frequency to avoid Wi-Fi. We develop a prototype of ChARM using srsRAN, and leverage the Colosseum channel emulator to collect a large-scale waveform dataset to train our neural networks with. To collect standard-compliant Wi-Fi data, we extended the Colosseum testbed using system-on-chip (SoC) boards running a modified version of the OpenWiFi architecture. Experimental results show that ChARM achieves accuracy of up to 96% on Colosseum and 85% on an over-the-air testbed, demonstrating the capacity of ChARM to exploit the considered spectrum channels.

## I. INTRODUCTION AND MOTIVATION

According to the new Cisco Annual Internet Report, 5G and beyond (NextG) networks will support more than 10% of the world’s mobile connections by 2023, with more than 5.7B users – 70% of the global population – using mobile cellular connectivity [1]. Due to this sheer growth in wireless demand, current spectrum bands below 6 GHz will inevitably become saturated. For this reason, the Federal Communication Commission (FCC) has recently opened 1.2 GHz of spectrum in the 6 GHz band, basically quadrupling the amount of space available for routers and other unlicensed devices [2]. Moreover, 150 MHz of spectrum in the Citizen Broadband Radio Service (CBRS) band can now be accessed [3], [4], shared with incumbent radar communications.

This article is based on material supported in part by the US National Science Foundations under the grants CNS #1923789 and #1925601, and by the US Office of Naval Research under grant ONR N00014-20-1-2132.

As new spectrum bands become open for unlicensed usage, it becomes crucial to protect incumbent users (*i.e.*, previous license owners), as well as establishing fair coexistence among unlicensed users. For example, it has been demonstrated that Wi-Fi throughput can drop up to 70% without a dedicated LTE co-existence mechanism [5]. To this end, *spectrum sharing* has emerged as a key technology to fuel wireless growth in these bands [6]. Spectrum sharing enables multiple categories of users to opportunistically select frequencies and bandwidth of operation, according to given constraints (e.g., band limits and incumbent priorities).

Due to the dynamic nature of spectrum policies and the unpredictability of unlicensed usage, spectrum sharing will require radio access networks (RANs) to change their operational parameters intelligently and according to the current spectrum context. Although existing RANs do not allow real-time reconfiguration, the fast-paced rise of the Open RAN movement and of the O-RAN framework [7] for 5G-and-beyond (NextG) networks, where the hardware and software portions of the RAN are logically disaggregated, will allow seamless reconfiguration and optimization of the radio components [8]. Despite their compelling necessity, to the best of our knowledge there are no O-RAN-ready technologies that can drive real-time RAN optimization, as discussed in details in Section II.

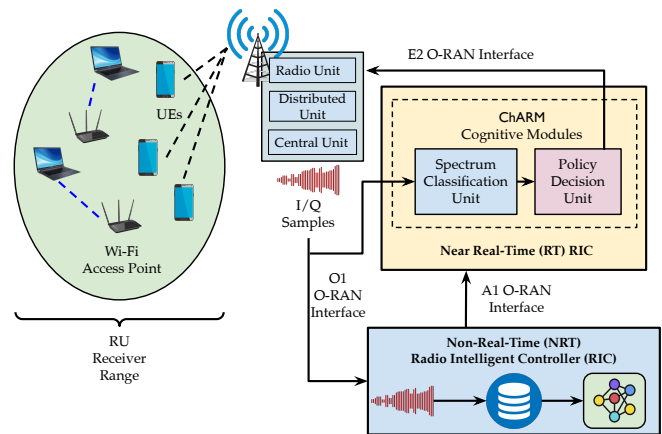


Fig. 1. Overview of the O-RAN-based ChARM spectrum-sharing framework.

For this reason, in this paper we propose the *Channel-Aware Reacting Mechanism* framework (in short, ChARM). Fig. 1 shows a high-level overview of ChARM and its main logical components, including the O-RAN interfaces used to collect and exchange data among the different components. ChARM

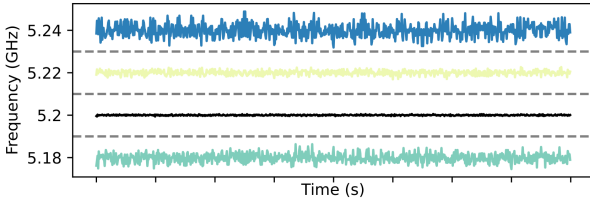


Fig. 2. Spectrum sensing based on different frequencies. The sensing bandwidth is set to 20 MHz (the LTE channel bandwidth in the ISM band). Some channels present radio signals, but their identification as legitimate communication or just noise requires a classifier.

is a data-driven framework that enables RAN owners to (i) sense the spectrum to understand the current context through a Spectrum Classification Unit (SCU); (ii) react in real time by switching the Distributed Unit (DU) and Radio Unit (RU) operational parameters according to a specified spectrum access policy decided by Policy Decision Unit (PDU). Both SCU and PDU are located in the O-RAN near-real-time RAN Intelligent Controller (RIC), which receives input by the non-real-time RIC. The latter is tasked with (i) collecting the spectrum I/Q data and creating a dataset; (ii) training and testing the machine learning (ML) algorithms that are eventually deployed onto the real-time RIC through the A1 interface.

The key innovation behind ChARM is providing Open RAN networks with the capability to intelligently determine which wireless technology is utilizing the spectrum, so that intelligent spectrum policies can be implemented. To this end, the SCU of ChARM leverages Deep Neural Network (DNN) trained on unprocessed I/Q samples to classify communication technologies with low latency [9]. Different from prior work, however, we design our classifiers to include an *abstain class* (see, for example, [10]) to minimize misclassifications of unknown wireless technologies (something likely in the Industrial Scientific Medical (ISM) band). Figure 2 shows an example of spectrum occupation in the ISM band between 5.18 and 5.24 GHz, where different wireless technologies are utilizing the spectrum. According to the given spectrum utilization rule, the PDU unit of ChARM may decide to switch to the empty 5.2 GHz band, also called inter-channel sharing, or activate a co-existence mechanism inside the occupied channel, such as (LTE-U, LTE-LAA or MulteFire). This methodology is called intra-channel sharing.

To the best of our knowledge, ours is the first framework providing the capabilities defined above to O-RAN-ready networks. The closest work to ours is due to Tarver *et al.* [3], who presented a solution for sensing and reacting nodes for the CBRS context, as well as Uyadov *et al.* [11], who propose a sensing and reacting framework optimizing the usage of fragmented, unused portions (holes) of spectrum. However, these approaches require deep modifications of the 3GPP and 802.11 standards, which ultimately makes them not readily adaptable to state-of-the-art O-RAN networks. Some solutions [12], [13] rely on a centralized orchestrating node, do not actively sense the state of the spectrum, or are inherently limited to two technologies (LTE and WiFi). Moreover, legacy approaches

do not allow the customization of the behavior by the Mobile Network Operator (MNO), and are not compatible with O-RAN specifications. Conversely, operators should be able to specify customized reactions tailored to the sensed technology and the band of operation.

As part of the novel contributions of this paper, we address (i) the need for a large waveform dataset to train the DNN with, and (ii) the development of a real-time working prototype. To experiment in both emulated and over-the-air channels, we develop a prototype for both the Colosseum channel emulator and the over-the-air Arena testbed. Colosseum enables researchers and practitioners to control the wireless channel environment while using state-of-the-art Software Defined Radio (SDR) devices. While Colosseum has not been designed to work with Wi-Fi devices, we extend Colosseum with new hardware in the loop, proving its extreme flexibility and extensibility. Our prototypes prove that ChARM is fully O-RAN-ready, it can interact with the 3GPP and 802.11 standards, and it is designed to be used in combination with any other intra-channel mechanisms.

To summarize, this paper makes the following novel technical contributions:

- We present ChARM, an O-RAN-based framework for spectrum sharing in the ISM band. ChARM is composed by (i) a spectrum classification unit (SCU) based on DNNs for real-time spectrum classification, (ii) a policy decision unit (PDU) that defines the actions to be taken upon the inference produced by the SCU;

- We design and implement a ChARM prototype based on standard-compliant srsRAN software. Through this prototype, we demonstrate ChARM in the context of spectrum sharing among LTE and Wi-Fi in unlicensed bands, where the RU reactively switches cell frequency to avoid Wi-Fi according to the DNN-based SCU inference. We leverage the Colosseum channel emulator to collect a large-scale waveform dataset to train our neural networks with. To collect standard-compliant Wi-Fi data, we extended the Colosseum testbed using System on Chip (SoC) boards, running our patched version of Open-WiFi [14], an 802.11a/g/n implementation specifically designed for SoC boards. We demonstrate the feasibility of our approach by deploying our software and the DNN model, trained on Colosseum, in a wireless test-bed, Arena [15], and operating it in the ISM band with incumbent WiFi communications. Experimental results show that our neural networks achieve accuracy of up to 96% on Colosseum and 85% on Arena, demonstrating the capacity of ChARM to exploit the considered spectrum channels;

- For reproducibility purposes and to stimulate further research, we provide access to our code and dataset (Section VI).

## II. RELATED WORK

A significant amount of prior work has tackled spectrum sharing in the ISM band, primarily targeting spectrum sharing between LTE and WiFi. Some approaches assume a collaboration between LTE and WiFi nodes; Chen *et al.* [16] envision the creation of a LTE/WiFi super node, internally optimizing the

spectrum usage fairness. Gawlowicz et al. [17] design a framework for side channel communication between WiFi access points and LTE Base Station (BS)s. These approaches, along with the one by Bocanegra et al. [5] that modifies the WiFi access point software, are challenging to deploy in practice, and hardly extensible to consider other technologies beyond LTE and WiFi. Some prior approaches achieve co-existence at the physical layer (PHY). The work by Yun et al. [18] focuses on interference cancellation and beamforming exploiting multiple radio antennas. Almeida et al. [19] focus on exploiting a 3GPP standard feature, the Almost Blank Subframe (ABS), and they paved the way for the standardization of LTE-U [20], originally proposed by Qualcomm, as a mean of intra-channel LTE co-existence. Guan and Melodia [21] mathematically modeled the fairness of LTE-U systems and proposed algorithms to maximize throughput under fairness constraints.

The solutions based on LTE-U could not be deployed in Europe and Japan, where regulations impose to use a Listen Before Talk (LBT) mechanism (CSMA/CA-like) to access the ISM band. Hence, 3GPP standardized another technique called LTE-LAA [22], which is an extension to LTE enabling LBT. Several works stemmed from this standardization effort; Chalhita et al. [23], and later, Tan et al. [24], propose to employ ML to forecast Wi-Fi transmission and optimize LTE consequently. Garcia Saavedra et al. [25] raised attention on LTE-LAA unfairness cases and propose optimizing parameters to minimize them; Gao and Roy [26] addressed instead the unfairness by modeling LTE-LAA communications with Markov models. The works by Chai et al. [27] and Saha et al. [28] introduce modifications to the LTE base station and the WiFi access point, respectively. Both these solutions and the ones based on LTE-U and LTE-LAA focus on intra-channel spectrum sharing. Huang et al. [29], instead, propose to achieve a fair co-existence between LTE and WiFi transmission by inter-channel optimization through a real-time intensive CUDA computation. Qian et al. [12] address the problem of centralized spectrum allocation among different MNOs. The approach by Mosleh et al. [13] presents an ML framework to optimize the spectrum usage by LTE and WiFi. However, it does not include sensing functions and its application is limited to those two technologies. Even though existing work tackles wireless technology classification through DNN [9], to the best of our knowledge, we are the first to propose a full-fledged O-RAN based framework for sensing and reacting cells, while maintaining full compatibility with the 3GPP standard.

### III. THE CHARM FRAMEWORK

#### A. Background on O-RAN

O-RAN and the NextG architecture are based on the 3GPP functional split. The functionalities of the base stations are virtualized and disaggregated, often running on multiple physical nodes. These functionalities are grouped in Central Unit (CU), DU, and RU. Specifically, while CU deals with protocols higher in the stack, DU is responsible for time-critical operations (including most baseband processing), while the RU is in

charge of radio frequency and of some Physical layer (PHY) functionalities (e.g., beamforming, fast Fourier transforms).

Moreover, O-RAN has been designed to embrace programmatic control based on ML and on the open source paradigm. For this reason, it exposes analytics and control knobs through the non real time RIC and the near real time RIC. These two components are responsible of the intelligent control of the network. The former handles operations with coarse time granularity (such as training a DNN model, orchestration of containers, among others), while the latter handles operations that need to be performed within a second, for example, the inference of a DNN model. The near real time RIC also allows running customized network functions (called xApps), which MNO can install in their nodes. ChARM has been specifically tailored to be deployed as an xApp in the near real time RIC and integrated in the NextG architecture.

#### B. Overview of ChARM

Figure 3 represents a high-level overview of the main logical components of ChARM in the context of O-RAN. The framework requires at least two co-located radios, one for mobile network communications (indicated with TX/RX), and another for sensing (indicated with RX). Moreover, ChARM is composed of (i) a spectrum classification unit (SCU) responsible of scanning various given frequencies and classify each of them, which comprises of a pre-defined set of frequencies to evaluate and a DNN for I/Q sample classification, (ii) a policy decision unit (PDU) which takes as input the latest frequency evaluation by the classifier, embeds a policy which can be customized by the operator (see Section III-D), and communicates to the DU unit the changes to apply to the on-going communication, and (iii) the DU, which implements the control interface to receive commands from the PDU.

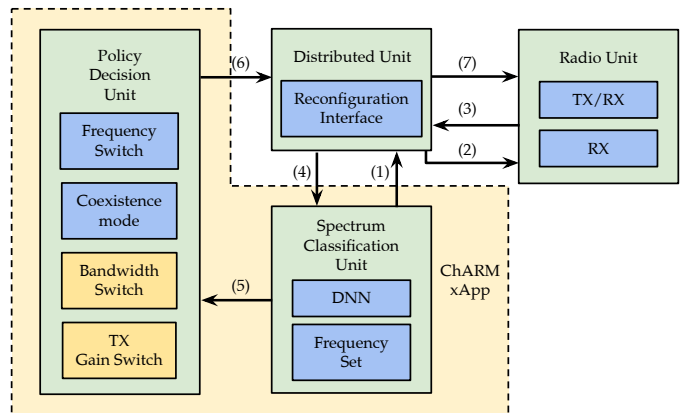


Fig. 3. ChARM system framework. Sub-blocks in the Policy Decision Unit indicate possible reacting strategies. While the framework is flexible enough to implement several different ones, for the purpose of this paper, we employ those highlighted in blue.

**A walk-through.** We provide an overview of the key operations of ChARM with the help of Fig. 3. While the RU can be communicating with zero or more User Equipments (UEs), the SCU periodically indicates to the DU (step 1) to reconfigure the RX radio to a different frequency (step 2). Then, the DU

collects I/Q samples (step 3), which are fed to the SCU (step 4). Then, the SCU classifies the samples through the DNN and the result (i.e., frequency and class) is provided to the PDU (step 5). The PDU is thus aware of (i) which frequency the RU is using for mobile communication, (ii) which is its latest assigned class, and (iii) the classes assigned to the other frequencies under sensing. The PDU may react to the sensed spectrum state triggering one or multiple of its functionalities, for example:

- Frequency switch, which makes the RU change center frequency;
- Coexistence mode, which enables or disables a specific coexistence mechanism of the RU;
- Bandwidth switch, which changes the signal bandwidth in the ISM band;
- TX gain switch, changes transmission gain of the RU.

The chosen reacting functions depend on the sensed spectrum state and the network operator policy (detailed in Section III-D), and they are sent to the DU (step 6). The DU adapts the spectrum usage with respect to the received commands (step 7). In the case of frequency or bandwidth switch, it communicates with the UEs through a 3GPP-standard compliant reconfiguration message [30] to grant the continuity of the ongoing communications.

### C. Spectrum Classification Unit

**Sensing Procedures.** Sampling a given frequency implies tuning the receiving radio and wait for the phase locked loop (PLL) to stabilize. This can take up to several tenths of seconds for each single channel to inspect. Alternatively, SDRs can be used to sense a larger portion of spectrum (multiple of channel width) and then filter out the channels of interest. While the latter does not present the inconvenience of frequency retuning, it has two main drawbacks: (i) state-of-the-art filtering, the polyphase channelizer [31], requires a large numbers of taps to be accurate, at the cost of being slower than retuning, and (ii) SDR maximum input bandwidth is constrained by hardware (e.g., 80 MHz on Ettus Devices USRP X310), which limits the sensing capabilities. Early experiments – not included due to space limitations – have shown the impracticability of the channelizer solution. For these reasons, ChARM employs a frequency hopping sensing mechanism.

**DNN.** I/Q samples represent a time series stream of data. Existing work has proven that Convolutional Neural Network (CNN)s are suitable for mining recurrent patterns and identifying key features in the wireless domain. CNNs have been used extensively for modulation and spectrum classification [32], [11]. However, in the computer vision field [33], and later in the audio processing [34], the concept of deep Residual Network (RN) has emerged and has been demonstrated to be increasingly effective. For example, RNs use convolutional layers and bypass connections, allowing the stacking of significant amounts of layers and the consequent effective analysis of data at many different scales. For this reason RNs have been applied to I/Q stream analysis too [35], and are considered in this paper.

### D. Policy Decision Unit

The goal of the PDU is to periodically collect the latest information generated by the classifier and, according to a given policy, instruct the DU on which spectrum changes to undertake. The policy is defined by an MNO to customize the PDU decisions, and it is bundled in the xApp. It is implemented as a function evaluating the current system state, defined by the classes assigned to the frequencies under evaluation, and the current communication frequency.

Algorithm 1 presents the periodic routine run by the Policy Decision Unit. Specifically, *ch\_classes* is an associative map, assigning to each sensed frequency by the SCU a technology label (e.g., {5.18 → Clear, 5.20 → LTE, 5.22 → Unknown}) generated by the DNN. The PDU periodic routine calls the policy function to determine the actions to perform. If the policy dictates a change of parameters, it triggers the respective operations of the DU reconfiguration interface.

---

#### Algorithm 1 Periodically run PDU algorithm

---

```

1: procedure PRI_UPDATE(ch_classes, curr_freq)
2:   freq, coex, pw, bw ← policy(ch_classes, curr_freq)
3:   if curr_freq ≠ freq then
4:     handover(freq)
5:   set_coexistence(coex)
6:   set_tx_power(pw)
7:   set_bw(bw)

```

---

**Frequency switch.** ChARM performs a handover whenever the PDU decides to change frequency. In this phase, it is crucial to guarantee continuity of the session and avoid disconnections of mobile UEs. 3GPP standards already indicate the procedure for inter-frequency handovers, and ChARM exploits it to grant standard compliant seamless handovers. ChARM RU manages two cells, one of them serving the UEs, while the other is kept idle. When ChARM changes operating frequency, (i) it changes the frequency of the idle cell with the target, and (ii) its DU sends a message handover through a RRC Reconfiguration Message [30] to the UEs.

**Co-existence mode.** ChARM targets spectrum sharing optimization both at the inter-channel level and at the intra-channel level. ChARM can hence work in two modes, co-existing and non co-existing. In non co-existing mode the PDU makes the network nodes communicate the regular way. When the PDU dictates a handover to a frequency already occupied, it can switch the DU to activate a predefined co-existence technique for the detected incumbent technology. Possible mechanisms include: the increase of Almost Blank Subframe periods [19], [21], [36] for the co-existence with WiFi, and the establishment of an X2 interface and the subsequent coordination through 3GPP Inter-Cell Interference Coordination (ICIC) techniques [37] for co-existence with LTE BSs. However, the specific choices for intra-channel spectrum sharing algorithms and performance are out of the scope of this paper, and we simply assume that, whenever a co-existence mode is required and activated, a sensible co-existence mechanism choice is set in place and the performance improves.

#### IV. CHARM PROTOTYPE

We first describe in Section IV-A the use-case scenario of ChARM we consider, as well as its design and implementation.

##### A. Use-case Scenario: Spectrum Sharing in ISM Bands

We cast ChARM in the context of spectrum sharing in the license-free industrial, scientific and medical (ISM) bands, where a 5G O-RAN cellular network (hereafter referred to as LTE for simplicity), Wi-Fi users and incumbent spectrum licensees need to share the same spectrum and thus coexist with each other. Figure 4 depicts the components of the ChARM prototype and their main interactions. We depict with a shade of blue and red, respectively, the interactions of ChARM with the channel: mobile communication and sensing. The image illustrates the inter-frequency spectrum optimization introduced in Section I; ChARM addresses that challenge by dynamically reconfiguring the mobile traffic to handover to the unoccupied sensed frequency.

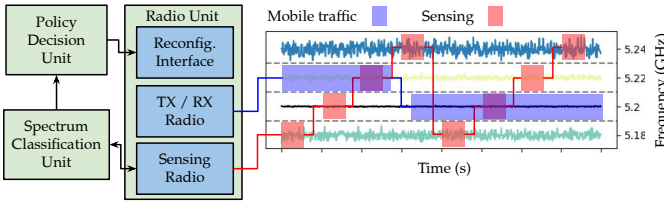


Fig. 4. View of the ChARM prototype components and their interactions.

In this scenario, the radio unit (RU) is composed by a reconfiguration interface, a sensing radio and a TX/RX radio. The sensing radio periodically listens to the channel and feeds the received waveform to the spectrum classification unit (SCU), which then sends its inference to the policy decision unit (PDU). The latter then interacts with the RU through the interface, which lets the TX/RX radio switch channel according to a given policy. In our experiments, we use a policy function based on a ranking of traffic classes. The two rankings we use in the shown experiments are presented in in Table I.

TABLE I  
CLASS RANKINGS TO BE USED FOR POLICY.  
HIGHER VALUES IMPLY HIGHER PREFERENCE.

(a)		(b)	
Clear	3	Clear	3
WiFi	2	WiFi	1
LTE	1	LTE	2
Unknown	0	Unknown	0

Algorithm 2 depicts our ranking-based policy function, whose goals are (i) to switch to more favorable frequencies according to the priority defined in Table I, and (ii) activate the LTE or WiFi co-existing mode if switching to an already occupied frequency. The activation/de-activation of the co-existing mode is depicted in Fig. 5.

Note that we purposely avoid to switch to a frequency whose incumbent technology is unknown to avoid unpredictable communication results. At line 2 of Algorithm 2, we determine the current classification for the frequency we use for the

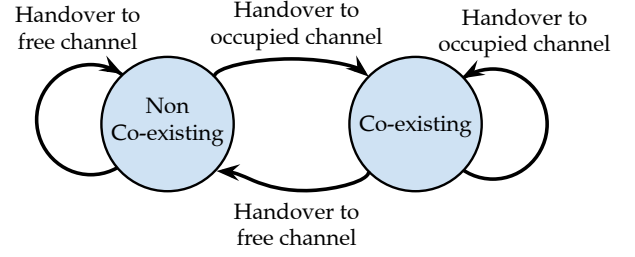


Fig. 5. Intra-channel co-existence. Transitions are consequences of handovers.

communication. Since the DNN classifies interference with the *unknown* class, as soon as our system detects unknown or WiFi communications on the currently used frequency (while in non co-existing mode), it reacts by switching channel, possibly switching also to co-existing mode. Conversely, if ChARM is in co-existence, and it detects a clear channel, it swiftly performs a handover to occupy it. Even if the framework includes functions for tweaking BS gain and bandwidth, we choose to use standard values for our experiments, as their use would unnecessarily complicate the policy logic for the purpose of this work.

##### Algorithm 2 Ranking-based policy used in the experiments.

```

1: procedure RANK_POLICY(channel_classes, curr_freq)
2:   curr_class ← get_class(channel_classes, curr_freq)
3:   if curr_class = (WiFi|Unknown) then
4:     freq, class ← max_{Table I}(channel_classes)
5:     if coexisting then ▷ currently in co-existence
6:       if class = CLEAR then
7:         return(freq, FALSE, std_gain, std_bw)
8:     else ▷ new interference detected
9:       if best_class = CLEAR then
10:        return(freq, FALSE, std_gain, std_bw)
11:      else if best_class ≠ UNKNOWN then
12:        if best_class = LTE then
13:          return(freq, LTE, std_gain, std_bw)
14:        else
15:          return(freq, WiFi, std_gain, std_bw)
16:    return(curr_freq, coexisting, std_gain, std_bw)

```

To classify unknown classes, we employ a classification mechanism for *abstain class* called *Entropy Selection (ES)*. ES is the simplest way to compute an uncertainty score for a prediction, by evaluating the entropy of the predicted probability. Our DNN outputs three numbers, which represent the probabilities of the input data to belong to, respectively, clear, LTE or WiFi channels. Let these probabilities be  $p_0, p_1, p_2$  respectively, then the entropy is defined as:

$$H = - \sum_{i=0}^2 p_i \log p_i \quad (1)$$

$H$  represents the uncertainty score, lower values mean our DNN is more confident of the classification. Validation of the model allows the selection of a hyper-parameter  $\alpha$ , and the classification is ultimately defined by:

$$\text{class} = \begin{cases} \arg \max_{i=0,1,2} p_i, & \text{if } H < \alpha \\ 3, & \text{otherwise.} \end{cases} \quad (2)$$

Where 0, 1, 2, 3 represents respectively the clear, LTE, WiFi and unknown classes. We implemented our prototype by leveraging srsRAN (<https://www.srsran.com/>), an extension of srsLTE [38]. We consider four frequencies (5.18, 5.20, 5.22, 5.24 GHz), equally spaced by 20 MHz, which coincide with the channels in the LTE band 46 and Wi-Fi channels. For this reason, we select 20 MHz as the bandwidth of the sensing radio. We extended the interface of srsRAN to support two additional commands (i) change the frequency of a specific cell; (ii) trigger the handover of the UEs from one specific cell to another.

### B. Colosseum Modifications and Data Collection

Training a DNN requires labelled ground-truth data that is realistic and as less affected by interference as possible. For this reason, we leveraged the Colosseum testbed to meet both requirements. In Colosseum, Commercial Off-The-Shelf (COTS) software can be deployed and run remotely; at the same time, the radio frequency channel is emulated, and real-world wireless communications can be elaborated while being protected from interference. Thanks to the Massive Channel Emulator (MCHEM) [39], Colosseum is a large-scale wireless network emulator, originally designed and deployed to support DARPA’s spectrum collaboration challenge in 2019. Colosseum servers and USRP SDRs allow researchers to experiment with wireless software and protocol stacks; in particular, Colosseum has already been employed for mobile networking with srsRAN [40].

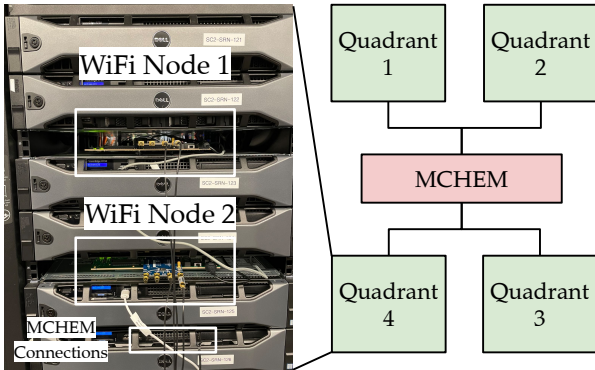


Fig. 6. Modifications to Colosseum for OpenWiFi devices.

On the other hand, the strict timing requirements of 802.11 channel access mechanisms such as CSMA prevent the compliant implementation of the 802.11 stack with SDRs [41]. In particular, 802.11 requires the reception of an acknowledgement packet for each frame sent, within 10  $\mu$ s from the frame successful transmission. To this end, we leveraged a Xilinx ZC706 [42], a SoC board fully supported by the OpenWifi project [14]. We worked with the Colosseum management team to deploy a hardware extension of Colosseum for working with WiFi nodes, depicted in Figure 6. This extension opens up new experiment opportunities for the whole research community working with 802.11 and spectrum sharing. The combination of the ZC706 and OpenWifi allows Colosseum to support fully compliant WiFi devices and communications.

As far as data collection is concerned, we collected three groups of spectrum data, namely background noise (clear), LTE data traffic, and WiFi data traffic. The data captures the general characteristic of LTE and WiFi transmissions, abstracting from the actual transmitted information, and throughput. We used srsRAN for cellular communications and OpenWifi for 802.11. We collected four classes of data:

- 1) Network with Idle traffic;
- 2) Continuous high-throughput traffic (iperf3, 1Mbps);
- 3) bursty high-throughput traffic (ping flooding, 1KB size);
- 4) bursty low-throughput traffic (ping, packets of 300 bytes).

The first class of data is meant to allow the DNN to learn of possibly idle base stations or access point that are not transmitting, but that could be potentially impacted by ChARM activity. The second and third class of data are meant to represent generic transmissions of random data. The fourth class is similar to the third, and it is used only for experiments as an evidence that ChARM is not over-fitting over a particular class of communication patterns, but it is able to extract the crucial wireless technology characteristics from the I/Q samples. Overall, the collected dataset consists of 172.8 GB of data, representing 43.2 billions of I/Q samples, and 18 minutes of communications. Note that we are not collecting samples for the “unknown” class. During data collection, we configured Colosseum to work at 5.24 GHz, and we used five of its nodes (two for LTE communication, two for WiFi communication, and another for data recording).

## V. EXPERIMENTAL EVALUATION

This section is logically divided in three parts. First, we present in Section V-A the experiments which have led to the ChARM DNN design for technology classification. Secondly, we showcase the ChARM prototype performance in the controlled Colosseum emulator environment in Section V-B. In particular, we detail the main features and behaviours ChARM can offer to mobile networking spectrum sharing. Lastly, we demonstrate the developed prototype of ChARM on an over-the-air, real-world environment through the use of the Arena testbed in Section V-C.

### A. DNN Training and Testing Procedures

As far as the training of the DNN is concerned, we adaptively stop the DNN training iterations whenever no sensible progress is gained for a large number of epochs. At the end, we save the network parameters with the best validation results. As in previous related research [35], we find the Adam optimizer to be a stable and effective choice, and we use it through our work. We split our dataset (described in Section IV-B) in the following way: 50% for training, 25% for validation, and 25% for testing.

**Test- $\alpha$  dataset and  $\alpha$  selection.** The ES method employed on the DNN for the abstain class requires the parameter selection for  $\alpha$  (see Section III-C). We create a new dataset, called test- $\alpha$ , consisting of the test set plus a combination of LTE traces, representing LTE interference (the latter accounting for the 25% of test- $\alpha$ ). While the test dataset is used to evaluate the accuracy of the resulting DNNs, the test- $\alpha$  dataset is used

to tune the parameter  $\alpha$ . Specifically, after we train our model using the training set, checking the accuracy on the validation set, we compute the value of  $\alpha$  which grants the higher accuracy score on the test- $\alpha$  dataset, and we use it consistently with our model when evaluating the test set.

**Model Selection.** Our investigation focuses on residual networks (RNs) and convolutional neural networks (CNNs). Since our prototype senses a bandwidth of 20 MHz, it receives a stream of 20M I/Q samples per second from the sensing radio. Therefore, when the DNN input size is 2,000, it represents one tenth of millisecond of communication, and, when it is 20,000, it represents one millisecond. Table II shows the two DNN architectures used throughout the paper, which were inspired by the work presented in [43].

TABLE II  
TWO DNN NETWORK LAYOUTS USED IN THIS WORK. CNN ARCHITECTURE (A) AND RN ARCHITECTURE (B).

Layer	Output dim.	Layer	Output dim.
Input	2 x 20000	Input	2 x 20000
Conv (ReLU)	7 x 20000	ResidualStack	4 x 10000
MaxPool	7 x 10000	ResidualStack	4 x 2000
Conv (ReLU)	7 x 10000	ResidualStack	4 x 1000
MaxPool	7 x 2000	ResidualStack	4 x 200
Conv (ReLU)	7 x 2000	ResidualStack	4 x 100
MaxPool	7 x 1000	ResidualStack	4 x 20
Conv (ReLU)	7 x 1000	ResidualStack	4 x 10
MaxPool	7 x 200	FC/Tanh	16
Conv (ReLU)	7 x 200	FC/Tanh	16
MaxPool	7 x 100	FC/Softmax	3
Conv (ReLU)	7 x 100		
MaxPool	7 x 20		
Conv (ReLU)	7 x 20		
MaxPool	7 x 10		
FC/Tanh	18		
FC/Tanh	16		
FC/Softmax	3		

We first evaluate how CNN and RN approaches perform against each other. Figure 7 shows the trade-off between input size and achieved accuracy by RN and CNN. In these experiments, we vary the number of hidden layers of the models according to the input size to grant always the finest degree of analysis (i.e., we do not increase the kernel size of the convolutional layers). During these experiments, RNs perform consistently better than CNNs and can reach an accuracy of 99% on our validation set. As expected, higher accuracy corresponds to a larger input size. We notice that 20,000 samples is representative enough to reach almost perfection on the validation set, without excessively impacting the processing time (sensing time is 1 millisecond, and processing time in the same order of magnitude). For the sake of clarity, the results shown here relate to RNs and CNNs with comparable number of parameters (about 3,000). The two network architectures achieving the highest accuracy are shown in Table II.

After selecting the network architecture and training the models, we tune the  $\alpha$  parameter. Figure 8 presents an analysis for parameter selection on the previously most successful models. The RN model achieves the best results with  $\alpha = 0.7$ , while the CNN model requires  $\alpha = 0.9$ . This difference means that RN is more confident on its prediction, hence, it

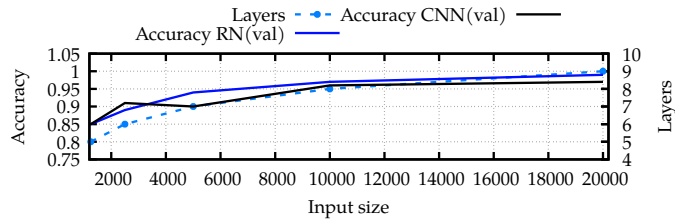


Fig. 7. Accuracy on the validation set for RN and CNN networks varying the input size.

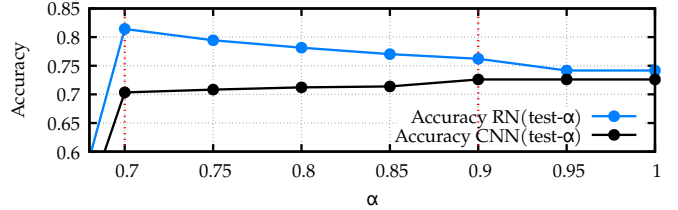


Fig. 8. Accuracy on the test- $\alpha$  set for RN and CNN models varying  $\alpha$ . Red lines intersect the maxima.

requires less account for uncertainty. Overall, the RN model obtains better performance and, for this reason, we select RN as our architecture of choice for ChARM. Figure 9 shows the performance variation when keeping input size to 20,000 while varying the number of layers, meaning opting for larger convolutional kernels. Results show there is little appreciable variation, except for the number of parameters, which increases with larger kernels. Our best RN model (architecture shown in Table II-B,  $\alpha = 0.7$ ) scores an accuracy of 96.4% on the test set. Table III shows the resulting confusion matrix for our model, and Table IV confirms that it is not biased toward any class.

### B. Sensing and Reacting

In this section, we demonstrate the spectrum optimization capabilities of ChARM. Specifically, we test ChARM in a controlled environment, so to be able to (i) emulate corner spectrum conditions, and (ii) obtain repeatable results. We leverage Colosseum since it enables fine-grained control over the wireless environment. In this section, we demonstrate that:

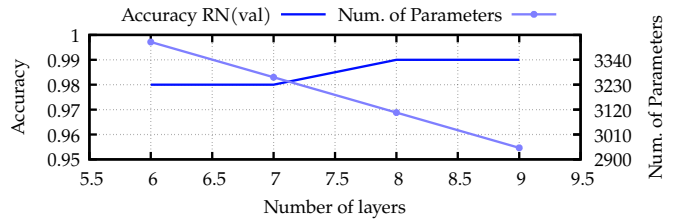


Fig. 9. Accuracy on the validation set for RN models varying the number of hidden layers.

TABLE III  
CONFUSION MATRIX OF OUR DNN ON THE TEST SET.

	Clear	LTE	WiFi	Unknown
Clear	87,202 (32.3%)	2 (0%)	110 (0%)	2,686 (1%)
LTE	3 (0%)	88,908 (32.9%)	104 (0%)	985 (0.4%)
WiFi	577 (0.2%)	152 (0.1%)	84,066 (31.1%)	5,205 (1.9%)

TABLE IV  
RECALL, PRECISION AND F1 MEASURES FOR OUR DNN ON THE TEST SET.

Technology	Recall	Precision	F1
Clear	0.9689	0.9934	0.981
LTE	0.9879	0.9983	0.9931
WiFi	0.9341	0.9975	0.9648

- (a) ChARM can detect interference with its communication,
- (b) it can perform a handover of the existing mobile communication to a different frequency,
- (c) it changes its mode to *co-existence* if switching to an already occupied frequency, and
- (d) its choices of frequency and whether to enable co-existence are close to the optimum (for a given policy).

The experiments start with the RU transmitting on the unoccupied 5.18 GHz channel, along with other two transmissions on 5.22 and 5.24 GHz. LTE and WiFi transmissions were recorded using Colosseum (4th class of the dataset, not used for training/validating/testing of the model) and are used in place of real nodes to make the experiment finely-controlled and reproducible. During the duration of the experiment, we keep an active communication between the ChARM BS and a srsRAN UE using a ping session. We log such continuous communication to check whether data is lost due to interference and handovers. We conduct extensive experimentation using Colosseum, varying the number of nodes and transmissions to stress ChARM. Here, we present results from two sessions that highlight all ChARM aspects, demonstrating claims (a)-(d).

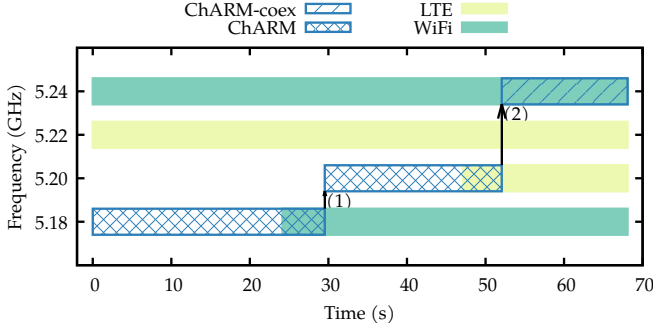


Fig. 10. Frequency occupancy during an experiment on Colosseum. Reported transmission classes are the ground-truth. Arrows indicate the triggering of handovers. The policy used is based on Table I-A

Figure 10 shows the channel transmissions during one of the experiments. Around the 24th second, an interfering WiFi transmission starts at frequency 5.18 GHz, the same that ChARM is using. It takes a few seconds – i.e., the overlapping boxed area in Figure 10 – for ChARM to detect interference and trigger a handover, indicated by arrow number 1. The detection of interference demonstrates claim (a), while the 3GPP standardized inter-cell handover guarantees continuity of the data communication between ChARM and the attached UE, demonstrating (b). ChARM handovers to frequency 5.2 GHz, which according to the policy defined by Table I-a, is the best choice, and does not require a co-existence mechanism. Around the 52nd second, an interfering LTE transmission starts on the same frequency

as ChARM. After a few seconds – shown in Fig. 10 with the second overlapping area – ChARM correctly detects interference with another LTE network and triggers a handover, indicated by arrow number 2. Claims (a) and (b) are further demonstrated, as ChARM detects the interference (a) and seamlessly perform a 3GPP handover (b). In this case, since there are no unoccupied frequencies among those under evaluation, ChARM follows the policy in Table I-a and switches to 5.24 GHz. Since ChARM detects an existing WiFi communication there, it activates the co-existence mode, hence demonstrating claim (c). It is worth noting that the choices performed by ChARM are optimal with respect to the policy. Besides the intervals for which the delay in channel sensing prevents the correct classification of channel occupancy, ChARM detects the correct underlying traffic, it switches to the expected frequency given the policy, and it activates the appropriate co-existence mode when needed, demonstrating claim (d).

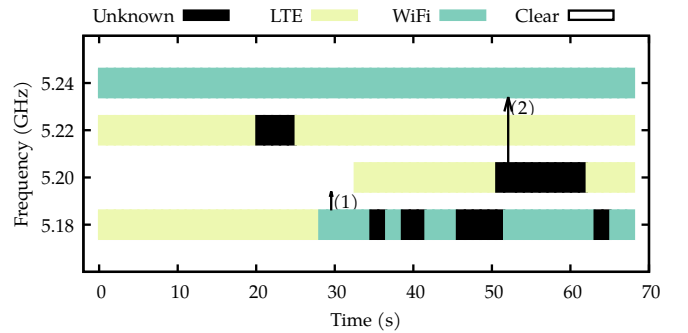


Fig. 11. ChARM DNN frequency classification through the experiment. Arrows indicate the triggering of handovers.

While Fig. 10 presents the objective development of the experiment, we show in Fig. 11 the classification outcomes of the DNN throughout the experiment. Specifically, we notice the interference detection, determining the triggering of the handovers (1,2), and some misclassification of LTE and WiFi communications as unknown technologies.

TABLE V  
CONFUSION MATRIX FOR CHARM CLASSIFICATION DURING AN EXPERIMENT.

	Clear	LTE	WiFi	Unknown
Clear	30 (11.2%)	0 (0.0%)	0 (0.0%)	0 (0.0%)
LTE	2 (0.7%)	106 (39.6%)	0 (0.0%)	14 (5.2%)
WiFi	0 (0.0%)	0 (0.0%)	76 (28.4%)	13 (4.9%)
Intrf	0 (0.0%)	8 (3.0%)	17 (6.3%)	2 (0.7%)

Table V presents the performance of the DNN during the experiment in terms of classification confusion matrix. As expected, the main source of misclassification stems from uncertainty in the interference and the abstain classes. Figure 12 presents another run showing the flexibility of ChARM, where Table I-b is enacted. In the spirit of O-RAN networks, we demonstrate that a simple change in the policy determines the preference of ChARM for co-existing with LTE technologies in place of WiFi, without any significant structural change.

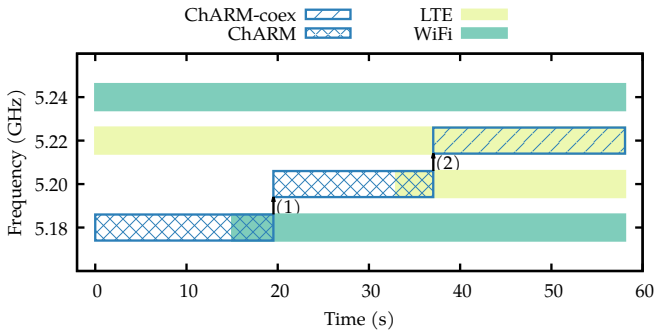


Fig. 12. Frequency occupation during an experiment on Colosseum. Reported transmission classes are the ground-truth. Arrows indicate the triggering of handovers. The policy used is based on Table I-B.

### C. Over-the-air Experimental Evaluation on Arena

We leveraged the Arena testbed [15] to perform over-the-air testing of ChARM. Arena is a remotely accessible and open test-bed made up of 64 SDRs and 8 servers designed for experimenting with 5G-and-beyond spectrum research. It allows the deployment and testing of communication platforms in a real office environment during working hours, subject to all sort of ISM interference. The antennas are installed in a large shared office, displaced along a grid, as represented in Fig. 13. The positioning in the grid of the nodes used in the experiments is also shown in the figure.

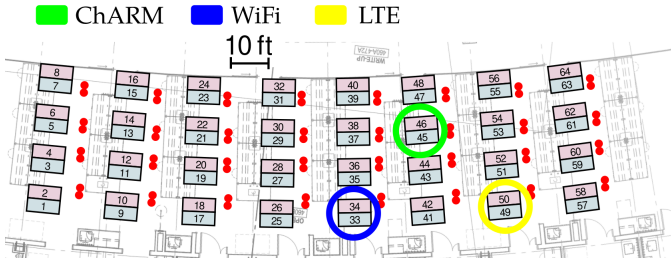


Fig. 13. Location of the wireless nodes in the Arena testbed.

While Colosseum allows experimenting in a fully controlled environment, Arena allows the testing of our system in a more realistic and challenging environment. Figure 13 presents the deployment of ChARM in Arena, including the location of the LTE and WiFi transmitting nodes. We choose 5.24 GHz as the center frequency. To generate the LTE and WiFi traffic, we use the traffic traces from our dataset. While the experiments on Colosseum show the behavior of ChARM and its ability to optimize the spectrum use, the experiments on Arena validate that the DNNs are still effective in a real-world environment. We emphasize that no data has been collected on Arena and used for the training of our model.

To compensate the path loss in Arena with respect to Colosseum, the transmissions are amplified by 10 dB. For the targeted LTE and WiFi transmission configurations (in terms of bandwidth parameters, LTE physical channel allocation, and WiFi modulation scheme) and transmission power, results shown in Fig. 14 confirm that ChARM can reliably detect the technologies obtaining an accuracy of 85%. Variations in the transmission

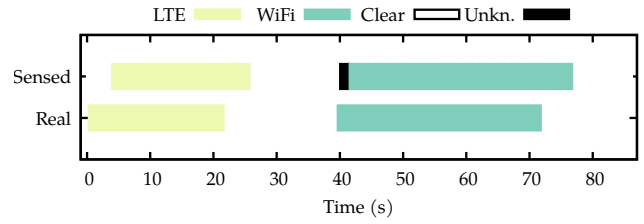


Fig. 14. Sensing experiment on the Arena test-bed at 5.24 GHz, with 20 MHz of bandwidth. We play out LTE and WiFi communication recordings (indicated as *Real* transmissions) and verify ChARM classification (*sensed*).

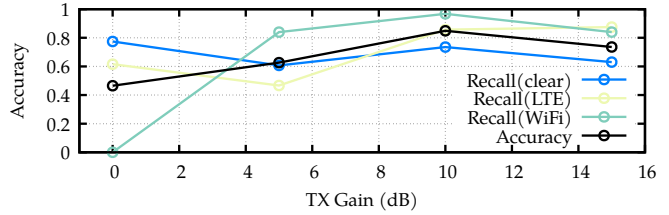


Fig. 15. Accuracy and recall of ChARM DNN obtained in the wireless test-bed for a single channel (5.24 GHz). The TX Gain is wrt the original transmission on Colosseum.

configuration or abrupt changes in the transmission power can however reduce our classifier performance, as shown in Fig. 15. Thus, it is important to tune the DNN training with respect to the target environment characteristics, and future work will investigate how online training can be used to automatically tailor the performance of ChARM.

## VI. CONCLUSIONS

In this paper, we have proposed Channel-Aware Reactive Mechanism (ChARM), a data-driven O-RAN-compliant framework that allows (i) sensing of the spectrum to understand the current context and (ii) reacting in real time by switching the distributed unit (DU) and RU operational parameters according to a specified spectrum access policy. It is designed to operate within the O-RAN specifications, and can be used in conjunction with other spectrum sharing mechanisms. We demonstrate the performance of ChARM in the context of spectrum sharing among LTE and Wi-Fi in unlicensed bands, where a controller operating over a RAN Intelligent Controller (RIC) senses the spectrum and switches cell frequency to avoid Wi-Fi. We develop a full-fledged standard-compliant prototype of ChARM using srsRAN, and leverage the Colosseum channel emulator to collect a large-scale waveform dataset to train our neural networks with. Experimental results show that our neural networks achieve accuracy of up to 96% on Colosseum and 85% on Arena, demonstrating the capacity of ChARM to fully exploit the considered spectrum channels.

The authors have provided public access to their code at [https://github.com/lucabaldesi/charm\\_code](https://github.com/lucabaldesi/charm_code) and to their dataset at <http://hdl.handle.net/2047/D20423481>

## REFERENCES

- [1] Cisco, "Cisco annual internet report (2018–2023) white paper," 2018. [Online]. Available: <http://tinyurl.com/zzo6766>

- [2] Federal Communications Commission (FCC), "FCC Opens 6 GHz Band to Wi-Fi and Other Unlicensed Uses," 2020.
- [3] C. Tarver, M. Tonnemacher, V. Chandrasekhar, H. Chen, B. L. Ng, J. Zhang, J. R. Cavallaro, and J. Camp, "Enabling a Use-or-Share Framework for PAL-GAA Sharing in CBRS Networks via Reinforcement Learning," *IEEE Transactions on Cognitive Communications and Networking*, 2019.
- [4] F. C. Commission *et al.*, "Amendment of the commission's rules with regard to commercial operations in the 3550-3650 mhz band," *GN docket*, 2015.
- [5] C. Bocanegra, T. E. Kennouche, Z. Li, L. Favalli, M. D. Felice, and K. Chowdhury, "E-Fi: Evasive Wi-Fi Measures for Surviving LTE within 5 GHz Unlicensed Band," *IEEE Transactions on Mobile Computing*, 2019.
- [6] Jeremy Horwitz, Venture Beat, "Wi-Fi 6E and 5G Will Share 6GHz Spectrum to Supercharge Wireless Data," 2020.
- [7] O-RAN Alliance, "White Paper: O-RAN: Towards an Open and Smart RAN," Tech. Rep., 2018.
- [8] L. Bonati, M. Polese, S. D'Oro, S. Basagni, and T. Melodia, "Open, Programmable, and Virtualized 5G Networks: State-of-the-art and the Road Ahead," *Computer Networks*, 2020.
- [9] M. Yang, Y. Song, C. Cai, and H. Gu, "Blind LTE-U/WiFi Coexistence System Using Convolutional Neural Network," *IEEE Access*, 2020.
- [10] Z. Liu, Z. Wang, P. P. Liang, R. R. Salakhutdinov, L.-P. Morency, and M. Ueda, "Deep Gamblers: Learning to Abstain with Portfolio Theory," in *Advances in Neural Information Processing Systems*, 2019.
- [11] D. Uyadov, Salvatore D'Oro, Restuccia, Francesco, and Melodia, Tommaso, "DeepSense: Fast Wideband Spectrum Sensing Through Real-Time In-the-Loop Deep Learning," in *IEEE INFOCOM 2021 - IEEE Conference on Computer Communications*, 2021.
- [12] B. Qian, H. Zhou, T. Ma, K. Yu, Q. Yu, and X. Shen, "Multi-Operator Spectrum Sharing for Massive IoT Coexisting in 5G/B5G Wireless Networks," *IEEE Journal on Selected Areas in Communications*, 2021.
- [13] S. Mosleh, Y. Ma, J. D. Rezac, and J. B. Coder, "Dynamic Spectrum Access with Reinforcement Learning for Unlicensed Access in 5G and Beyond," in *2020 IEEE 91st Vehicular Technology Conference*, 2020.
- [14] X. Jiao, W. Liu, M. Mehari, M. Aslam, and I. Moerman, "OpenWiFi: a free and open-source IEEE802.11 SDR implementation on SoC," in *2020 IEEE 91st Vehicular Technology Conference*. IEEE, 2020.
- [15] L. Bertizzolo, L. Bonati, E. Demirors, A. Al-shawabka, S. D'Oro, F. Restuccia, and T. Melodia, "Arena: A 64-antenna SDR-based Ceiling Grid Testing Platform for Sub-6 GHz 5G-and-Beyond Radio Spectrum Research," *Computer Networks*, Jul. 2020.
- [16] Q. Chen, G. Yu, and Z. Ding, "Optimizing Unlicensed Spectrum Sharing for LTE-U and WiFi Network Coexistence," *IEEE Journal on Selected Areas in Communications*, 2016.
- [17] P. Gawlowicz, A. Zubow, and A. Wolisz, "Enabling Cross-technology Communication between LTE Unlicensed and WiFi," in *IEEE INFOCOM 2018 - IEEE Conference on Computer Communications*, 2018.
- [18] S. Yun and L. Qiu, "Supporting WiFi and LTE co-existence," in *2015 IEEE Conference on Computer Communications (INFOCOM)*, 2015.
- [19] E. Almeida, A. M. Cavalcante, R. C. D. Paiva, F. S. Chaves, F. M. Abinader, R. D. Vieira, S. Choudhury, E. Tuomaala, and K. Doppler, "Enabling LTE/WiFi coexistence by LTE blank subframe allocation," in *2013 IEEE International Conference on Communications (ICC)*, 2013.
- [20] I. Qualcomm Technologies, "Qualcomm ResearchLTE in Unlicensed Spectrum: Harmonious Coexistence with Wi-Fi."
- [21] Z. Guan and T. Melodia, "CU-LTE: Spectrally-Efficient and Fair Coexistence Between LTE and Wi-Fi in Unlicensed Bands," in *Proc. of IEEE Conference on Computer Communications (INFOCOM)*, San Francisco, CA, USA, Apr. 2016.
- [22] 3GPP r13, "Study on Licensed-Assisted Access to Unlicensed Spectrum," 3GPP, Tech. Rep., 2015.
- [23] U. Challita, L. Dong, and W. Saad, "Proactive Resource Management for LTE in Unlicensed Spectrum: A Deep Learning Perspective," *IEEE Transactions on Wireless Communications*, 2018.
- [24] A. Garcia-Saavedra, P. Patras, V. Valls, X. Costa-Perez, and D. J. Leith, "ORLA/OLAA: Orthogonal Coexistence of LAA and WiFi in Unlicensed Spectrum," *IEEE/ACM Transactions on Networking*, 2018.
- [25] J. Tan, S. Xiao, S. Han, Y. Liang, and V. C. M. Leung, "QoS-Aware User Association and Resource Allocation in LAA-LTE/WiFi Coexistence Systems," *IEEE Transactions on Wireless Communications*, 2019.
- [26] Y. Gao and S. Roy, "Achieving Proportional Fairness for LTE-LAA and Wi-Fi Coexistence in Unlicensed Spectrum," *IEEE Transactions on Wireless Communications*, 2020.
- [27] E. Chai, K. Sundaresan, M. A. Khojastepour, and S. Rangarajan, "LTE in Unlicensed Spectrum: Are We There Yet?" in *Proceedings of the 22nd Annual International Conference on Mobile Computing and Networking*, New York, NY, USA, 2016.
- [28] S. K. Saha, C. Vlachou, D. Koutsonikolas, and K.-H. Kim, "DeMiLTE: Detecting and Mitigating LTE Interference for Enterprise Wi-Fi in 5 GHz," in *Proceedings of the Twentieth ACM International Symposium on Mobile Ad Hoc Networking and Computing*, New York, NY, USA, 2019.
- [29] H. Huang, S. Guo, G. Gui, Z. Yang, J. Zhang, H. Sari, and F. Adachi, "Deep Learning for Physical-Layer 5G Wireless Techniques: Opportunities, Challenges and Solutions," *IEEE Wireless Communications*, 2020.
- [30] 3GPP Release 10, "Radio Resource Control (RRC); Protocol specification," 3GPP, Tech. Rep., 2009.
- [31] F. Harris, C. Dick, and M. Rice, "Digital receivers and transmitters using polyphase filter banks for wireless communications," *IEEE Transactions on Microwave Theory and Techniques*, 2003.
- [32] T. J. O'Shea, J. Corgan, and T. C. Clancy, "Convolutional radio modulation recognition networks," in *Engineering Applications of Neural Networks*, C. Jayne and L. Iliadis, Eds. Cham: Springer International Publishing, 2016.
- [33] K. He, X. Zhang, S. Ren, and J. Sun, "Deep residual learning for image recognition," in *Proceedings of the IEEE Conference on Computer Vision and Pattern Recognition (CVPR)*, June 2016.
- [34] A. van den Oord, S. Dieleman, H. Zen, K. Simonyan, O. Vinyals, A. Graves, N. Kalchbrenner, A. Senior, and K. Kavukcuoglu, "Wavenet: A generative model for raw audio," 2016.
- [35] T. J. O'Shea, T. Roy, and T. C. Clancy, "Over-the-air deep learning based radio signal classification," *IEEE Journal of Selected Topics in Signal Processing*, 2018.
- [36] C. Cano, D. J. Leith, A. Garcia-Saavedra, and P. Serrano, "Fair Coexistence of Scheduled and Random Access Wireless Networks: Unlicensed LTE/WiFi," *IEEE/ACM Transactions on Networking*, 2017.
- [37] C. Kosta, B. Hunt, A. U. Quedus, and R. Tafazolli, "On interference avoidance through inter-cell interference coordination (icic) based on ofdma mobile systems," *IEEE Communications Surveys Tutorials*, 2013.
- [38] I. Gomez-Migueluez, A. Garcia-Saavedra, P. D. Sutton, P. Serrano, C. Cano, and D. J. Leith, "srsLTE: An open-source platform for LTE evolution and experimentation," in *Tenth ACM International Workshop on Wireless Network Testbeds, Experimental Evaluation, and Characterization*, 2016.
- [39] A. Chaudhari and M. Braun, "A Scalable FPGA Architecture for Flexible, Large-Scale, Real-Time RF Channel Emulation," in *2018 13th International Symposium on Reconfigurable Communication-centric Systems-on-Chip (ReCoSoC)*, 2018.
- [40] L. Bonati, S. D'Oro, S. Basagni, and T. Melodia, "SCOPE: An Open and Softwarized Prototyping Platform for NextG Systems," in *Proc. of ACM Intl. Conf. on Mobile Systems, Applications, and Services (MobiSys)*, Virtual Conference, June 2021.
- [41] B. Bloessl, M. Segata, C. Sommer, and F. Dressler, "An IEEE 802.11a/g/p OFDM Receiver for GNU Radio," in *Proceedings of the Second Workshop on Software Radio Implementation Forum*. New York, NY, USA: Association for Computing Machinery, 2013.
- [42] Xilinx Inc., "ZC706 Evaluation Board for the Zynq-7000 XC7Z045 All Programmable SoC User Guide," [https://www.xilinx.com/support/documentation/boards\\_and\\_kits/zc706/ug954-zc706-eval-board-xc7z045-ap-soc.pdf](https://www.xilinx.com/support/documentation/boards_and_kits/zc706/ug954-zc706-eval-board-xc7z045-ap-soc.pdf), 2018.
- [43] T. J. O'Shea, T. Roy, and T. C. Clancy, "Over-the-air deep learning based radio signal classification," *IEEE Journal of Selected Topics in Signal Processing*, 2018.